

A Multi-Function Common Mode Choke Based on Active CM EMI Filters for AC/DC Power Converters

LIYU DAI¹, (Student Member, IEEE), WENJIE CHEN¹, (Member, IEEE),
XU YANG¹, (Member, IEEE), MINGHUA ZHENG², YANG YANG¹, AND RUI WANG¹

¹Department of Electrical Engineering, Xi'an Jiaotong University, Xi'an 710049, China

²Omron (China) Co., Ltd., Shanghai 200241, China

Corresponding author: Wenjie Chen (cwj@mail.xjtu.edu.cn)

This work was supported by Omron (China) Co., Ltd.

ABSTRACT It is widely believed that hybrid electromagnetic interference (EMI) filter (HEF) is one of the most optimized solutions for EMI elimination. Nevertheless, the desire for a smaller and lighter filtering method has never stopped. To further reduce the size and weight of a hybrid EMI filter, this paper proposes a multi-function common mode choke (MCMC) used in HEF. It differs from the traditional common mode (CM) choke in that two functions of (1) CM signal sensing and (2) CM noise suppression are integrated into one choke. In such a proposed MCMC design, the traditional current transformer (CT) is eliminated in the hybrid filter topology. This technique could reduce the size, weight, and cost of the filter to a great extent. Based on the MCMC, a novel CM filter is proposed to achieve high-performance noise suppression. System model and stability feature of the new filter are developed and investigated in detail. A filter prototype based on the proposed MCMC is constructed. It is tested on a 100-W commercial ac/dc converter. The experimental results show that the proposed CM filter can provide better EMI noise suppression with a smaller size. The insertion loss could reach 50 dB at low frequencies and 40 dB at high frequencies.

INDEX TERMS Hybrid EMI filter, common mode choke, modeling, electromagnetic interference (EMI).

I. INTRODUCTION

As we know, power electronics equipment such as switched-mode power supplies (SMPS) or inverters generate high frequency conducted electromagnetic interference (EMI) noise due to the fast switching currents di/dt and voltages du/dt [1]–[3]. Therefore, EMI filters have been widely used for years to tackle conducted EMI problems for electronic applications. Generally, passive EMI filters (PEF) [2]–[5], [18], active EMI filters (AEF) [6]–[13] and passive/active hybrid EMI filters (HEF) [11], [13]–[16], [22] are the three kinds of EMI filters at present.

Passive EMI filters, which are composed of inductors and capacitors, are the most commonly used solutions for their simplicity and reliability [2]. However, they suffer from such disadvantages as bulky, heavy and unacceptable component loss [3], [4]. These make them difficult to satisfy the critical design requirements of power electronics equipment.

The associate editor coordinating the review of this manuscript and approving it for publication was Snehal Gawande.

To tackle these problems, active EMI filters are introduced to meet the increasing demand for high power density equipment. In general, AEFs consist of three parts: a sensing unit, an amplification unit and an injection unit. An active EMI filter can sense and inject either voltage signal or current signal to reduce the noise. There are mainly four different topologies of active EMI filters according to what is sensed and what is injected [8], [10]. The facts that active EMI filters can reduce low-frequency EMI noise effectively and provide alternative approaches to the EMI problems have been proved by a large number of researchers [1]–[18]. But the performance of high-frequency noise attenuation is still not good enough due to the component bandwidth limitation.

To combine the advantages of both passive filters and active filters, the passive/active hybrid EMI filter becomes another solution. Since hybrid EMI filters can achieve complementary advantages of passive filters and active filters, it has broader application prospects to provide an alternative approach both from the technical level and from the feasibility level. During the last decade, various hybrid filters

have been put forward and applied in DC/DC converters [4], [9], [10], [21], [25], AC/DC converters [14], [27], [32], [33], motor drive systems [5]–[7], [12], [16], [17] etc. Di Piazza *et al.* studied the hybrid EMI filter structure and used it in a motor drive system [7]. Shin *et al.* reported a compact transformerless CM EMI filter using a push–pull amplifier, and also presented the design guidelines for active EMI filter in a compact package [15]. With the development of magnetic integration technique, Switzerland researchers Biela *et al.* [18] reported a high density integrated hybrid EMI filter. Recently, the digital active EMI filters used in a Grid-Tied PV Microinverter Module and switch mode power converters were reported in [19]–[21]. These publications are very important to EMI filter research. Nevertheless, it is widely believed that this line of research has not yet reached its maturity.

Firstly, the desire for smaller and lighter products has never stopped in electrical engineers. As we know, passive components like CM choke or DM choke are still one of the biggest unit in EMI filters. To reduce that part, Chen *et al.* [11] reported a method of active impedance multiplication using a hybrid CM filter. Therefore, the total equivalent impedance was enlarged by current-sense current-injection active circuit. Only a small-size CM choke was used as the passive filter. Chu *et al.* introduced a modeling method to analyze the performance of the hybrid EMI filter with several small passive components [3]. In general, how to achieve an accurate design and to reduce the size and weight of filter components are still the main challenge for hybrid EMI filters researchers.

Meanwhile, from the concept of HEF appeared to the present, for the hybrid filter, active circuit and passive circuit are always treated as two separated parts. On the one hand, the circuit structures of the two parts are independent of each other. On the other hand, the circuit functions of the two parts also do not affect each other. The disadvantage is obviously that two parts of the circuit operate independently. Both circuits lack coordination with each other, which, in turn, results in the whole volume and weight of the filter become too large.

On considering the problems mentioned above, a multi-function common mode choke (MCMC) is proposed in this paper. The proposed MCMC integrates two functions of both CM signal sensing and CM noise suppression. By designing the reasonable parameters, it can optimize the function of hybrid EMI filter, and achieve miniaturization of HEF at the same time. In this scheme, the novelty can be listed as follows.

1) A new integrated MCMC based on HEF is proposed, which combine CM signal sensing function and CM noise suppression function into one component. By means of the proposed MCMC, traditional current transformer is eliminated. Hence, the topology of hybrid EMI filter can be optimized.

2) The two functions of the proposed MCMC are studied thoroughly. Equivalent models of CM noise suppression function and CM signal sensing function are developed in detail. For the CM noise suppression, a decoupled model is derived to calculate the equivalent CM impedance of the

proposed MCMC. For the CM signal sensing function, three significant properties, transimpedance $G_{CT}(s)$, phase error θ and low cut-off frequency f_L are analyzed in detail based on the developed model. In addition, the selections of key parameters are taken into full consideration, which presents a design guideline for the proposed MCMC.

3) A prototype of the novel EMI filter based on the proposed MCMC is designed and constructed, which realizes a miniaturization of the hybrid EMI filter. In addition, comparative experiments between the new CM filter proposed in this paper and the traditional hybrid active EMI filter are carried out to verify the effectiveness of the proposed technique.

The proposed technique benefits from the following advantages:

- Miniaturization and lightweight;
- Only design a magnetic component, simplify the design process, without the concern of coupling and interference problems between the two magnetic components;
- Achieve better CM noise suppression;
- No influence on the design of the DM filter.

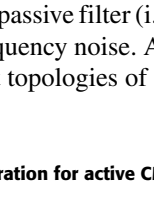
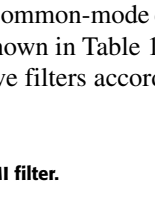
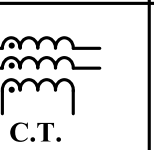
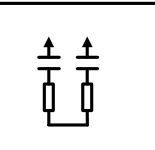
The rest of this paper is organized as follows. The design motivation and structure of the multi-function common mode choke is introduced in section II. The models of two functions (CM signal sensing and CM noise suppression) are developed and analyzed in section III. The design procedure of the new filter based on the proposed MCMC is presented in section IV. The experimental results and comparisons are shown in section V to validate the proposed technique. Further considerations are given in section VI. Section VII is the conclusion of this paper.

II. PROPOSED MULTI-FUNCTION COMMON MODE CHOKE

A. IDEA OF THE PROPOSED MULTI-FUNCTION COMMON MODE CHOKE

A hybrid filter is composed of an active filter and a passive filter. While the active filter is designed to attenuate the low-frequency noise, the passive filter (i.e., common-mode choke) reduces the high frequency noise. As shown in Table 1, there can be four different topologies of active filters according to

TABLE 1. Circuit configuration for active CM EMI filter.

	Sensing	Injection
Voltage		
Current		

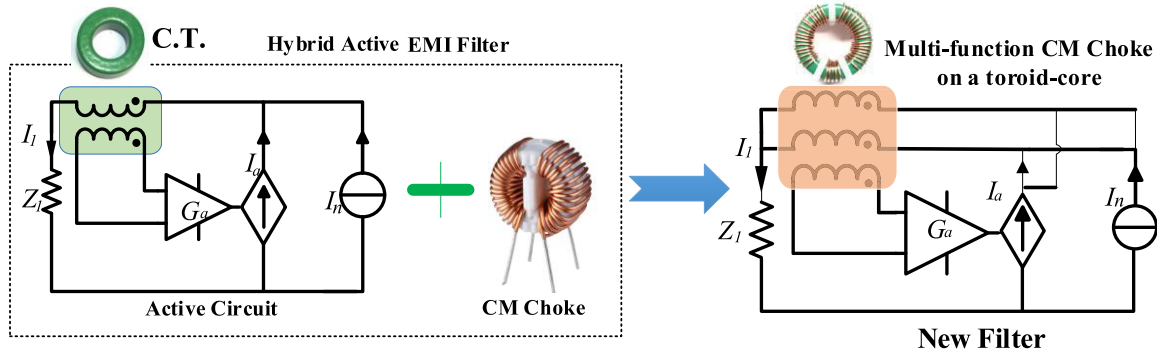


FIGURE 1. Idea of the proposed multi-function common mode choke.

what is sensed and what is injected. For injection part, there are two ways to reduce CM noise, voltage compensation and current cancellation. While voltage compensation needs one voltage transformer that is generally big. Because the full line currents must flow through its primary windings and lead to extra power loss in active filters. Therefore, voltage compensation is not preferred. For the noise sensing, the active filter can sense either voltage or current, but current sensing is preferred over voltage sensing. Because current sensing employs a current transformer and it is convenient to sense the CM noise current. Moreover, the current transformers can introduce additional gains for the whole system as compared to voltage sensing [11], [26].

Based on the analysis above, current sensing-current canceling active CM filter topology is effective in eliminating the CM noise. However, it employs a current transformer to sense the CM noise, which obviously takes up additional space, of course, costs more. Therefore, in the hybrid active filter, the idea that current transformer integrates into CM choke comes into being. In this paper, a multi-function common mode choke is proposed in which the current transformer and the common choke are combined into a single component. In such a proposed multi-function common mode choke design, the current transformer can be eliminated.

However, in the traditional hybrid active filter, the two discrete components current transformers and CM chokes can be flexibly designed as required. Their functions are independent and unable to affect each other. But the challenge how to ensure that two functions can be realized through ingenious designs exists for the proposed MCMC. On the one hand, MCMC need to achieve the function of accurate noise current sensing. On the other hand, the large enough CM impedance is required to serve as a passive filter. What's more, to design a stable system based on the MCMC is also a challenge because of the new topology.

B. STRUCTURE OF THE NEWLY PROPOSED MULTI-FUNCTION COMMON MODE CHOKES

The structure of the proposed multi-function common mode choke is shown in Fig. 2. It consists of two traditional CM

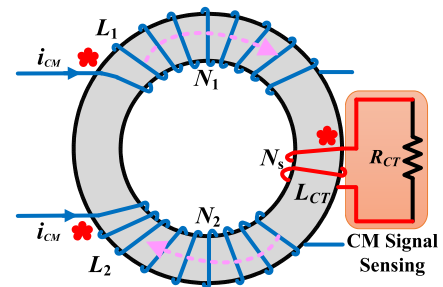


FIGURE 2. Structure of the newly proposed multi-function common mode choke.

inductor windings for the converter’s main power paths and a CM current sensing winding connected to a sense resistor R_{CT} . L_i ($i = 1, 2, CT$) are the inductance for the three windings. All the windings are wound on the same magnetic core. The two windings (L_1 and L_2) are designed to be identical and symmetrical. Briefly speaking, the principle of this multi-function common mode choke is to add a third sensing winding achieving CM noise current sensing. In addition, the CM impedance of each main winding is possible not to be affected through ingenious design consideration.

III. MODELING OF THE MULTI-FUNCTION COMMON MODE CHOKES

A. MODELING OF THE CM SIGNAL SENSING FUNCTION

As discussed previously, the two primary windings which have the same number of turns are connected to main power paths of a converter. They are in parallel and the CM noise currents will generate signals in the third sensing winding while the magnetic fluxes generated by DM currents cancel each other. Because of this, the CM signal sensing function of the MCMC can be modeled as a two-port network as shown in Fig. 3 [23]. Where C_p and C_s are the parasitic capacitance of the primary and the secondary windings; C_{ps} is the interwinding capacitance between the primary and the secondary windings; L_{lp} and L_{ls} are the leakage inductance of the primary and the secondary windings; R_p and R_s are the resistances of the primary and the secondary windings; R_C is

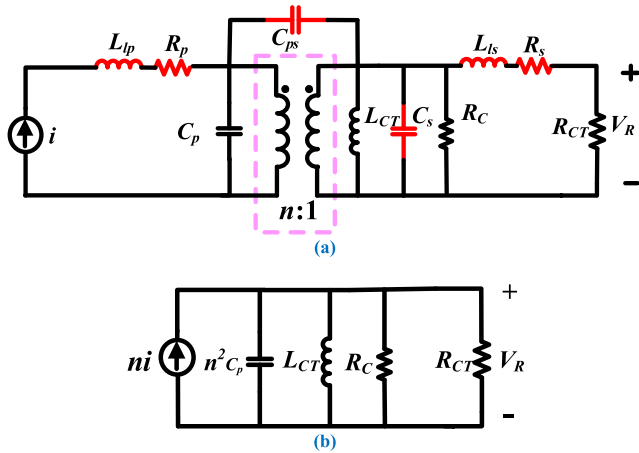


FIGURE 3. CM signal sensing model: (a) Model with parasitic components. (b) Simplified model with the current source reflected to secondary.

the parallel equivalent resistance, representing the core loss; L_{CT} is the magnetizing inductance on the secondary side; R_{CT} is the sense resistor.

Different from the conventional current transformer used in the active EMI filter, in the structure of multi-function common mode choke, the primary winding has many turns (i.e., ten or more) to acquire enough inductance. The enough inductance is needed for the CM noise suppression function. While the secondary winding has few turns and its turn is $n:1$ ($n = \frac{N_1}{N_s}$). As a consequence, primary parasitic capacitance C_p is not so small as to be negligible. In addition, it is reflected to the secondary side, where it is increased by a factor of n^2 . Therefore, the effect of C_p can't be ignored.

The multi-function common mode choke uses a high permeability ferrite core ($\mu_r = 6700$), which leads to a small leakage inductance (measured as 364 nH) on the third sensing winding. The impedance of the leakage inductance is much smaller than the load resistance 300 Ω within the concerned frequency range from 150 kHz to 30 MHz. C_s is much smaller than $n^2 C_p$. Based on the analysis above, C_s , L_{lp} , L_{ls} , R_p , R_s , and C_{ps} can be ignored in the model of CM signal sensing function [23]. Hence, the simplified model with the current source reflected to secondary can be obtained as shown in Fig. 3(b).

For the CM signal sensing function, there are mainly three significant properties to be considered as follows:

1) TRANSIMPEDANCE $G_{CT}(s)$

The transimpedance of the current transformer is given by the relation

$$G_{CT}(s) = \frac{V_R(s)}{I(s)} \quad (1)$$

where $V_R(s)$ and $I(s)$ are the Laplace transforms of the voltage across the sense resistor R_{CT} and the sensing current in the primary side, respectively. Based on the simplified model,

the transimpedance $G_{CT}(s)$ can be derived as

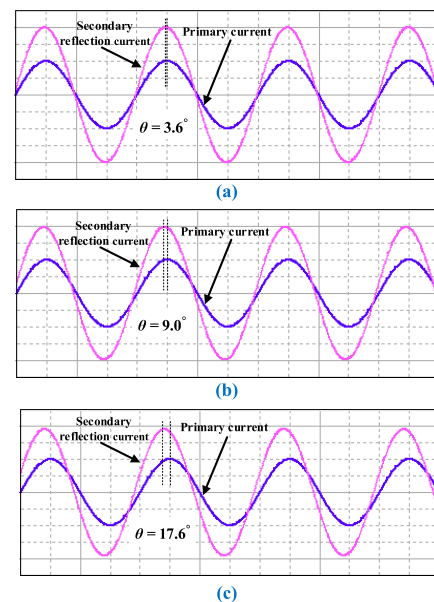
$$G_{CT}(s) = \frac{V_R(s)}{I(s)} = n \cdot \frac{sL_{CT}R_C R_{CT}}{s^2 L_{CT}R_C R_{CT} n^2 C_p + sL_{CT}(R_C + R_{CT}) + R_C R_{CT}} \quad (2)$$

2) PHASE ERROR θ

The phase error θ between the secondary reflection current and primary current can be derived as

$$\theta = \arctan \frac{R_{CT}}{2\pi f L_{CT}} \quad (3)$$

Phase error of CM signal sensing will affect the compensation of the active filter. The relation is used for qualitative analysis, which also provides one design consideration when designing the MCMC. Fig. 4 shows the primary current and secondary reflection current signals when the third sensing winding connects to different sense resistors R_{CT} in the multi-function common mode choke. It can be found that the phase error is negligible at 200 Ω and 500 Ω but become significant at 1000 Ω . Note that the phase error is concerned in the given examples and the amplitude relation between them depending on transimpedance $G_{CT}(s)$ is not in discussion under the topic of phase error. It can be concluded that larger sense resistor R_{CT} will result in heavier phase error when the magnetizing inductance remains constant.



(Scales: Horizontal: 0.5us/div; Vertical: 50mA/div)

FIGURE 4. Phase error of CM signal sensing at different sense resistors: (a) Phase error at 200 Ω . (b) Phase error at 500 Ω . (c) Phase error at 1000 Ω .

3) LOW CUT-OFF FREQUENCY f_L

CM signal sensing is required to have adequate bandwidth so that it can regenerate the sensed current. Based on the sim-

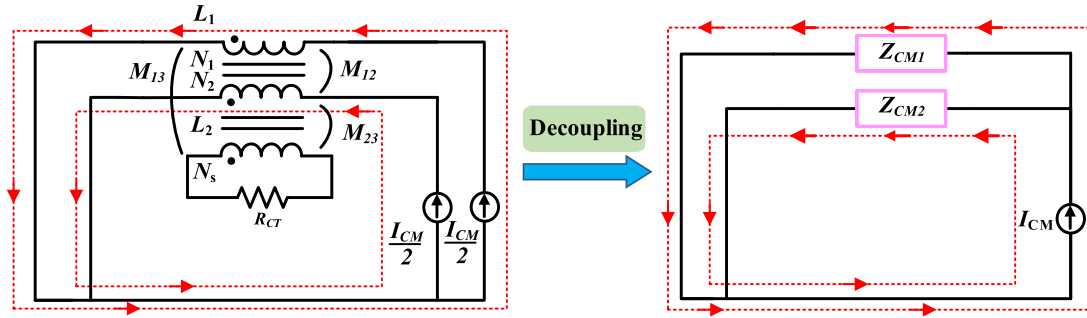


FIGURE 5. Modeling of CM noise suppression function.

plified CM signal sensing model, the low cut-off frequency can be determined by the value of the secondary winding impedance and its sense resistance as shown in equation (4).

$$f_L = \frac{R_{CT}}{2\pi L_{CT}} \quad (4)$$

Note that $n^2 C_p$ presents very high reactance at low frequency. R_C representing the core loss is very large relative to sense resistor R_{CT} . Hence, they can be ignored in the analysis of the low cut-off frequency. Concerning the low cut-off frequency, there are two aspects to consider during the design process. On the one hand, the low cut-off frequency should be lower than 150 kHz which is a lower frequency limit for conducted EMI test standard. On the other hand, the low cut-off frequency should not be too small to sense power frequency signals or low order harmonics.

B. MODELING OF THE CM NOISE SUPPRESSION FUNCTION

The CM noise suppression function of the proposed multi-function common mode choke can be modeled as shown in Fig. 5. The two windings (L_1 and L_2) that have the same number of turns ($N_1 = N_2$) act as the conventional CM choke windings while the sensing winding (L_{CT}) has only few turns in the design of MCMC. The equivalent CM impedance of the choke is used to estimate the CM noise suppression function. To analyze the equivalent CM impedance of the choke, the following equations in general form hold:

$$\begin{cases} V_1 = sL_1 I_1 + sM_{21} I_2 + sM_{31} I_3 \\ V_2 = sM_{12} I_1 + sL_2 I_2 + sM_{32} I_3 \\ V_3 = sM_{13} I_1 + sM_{23} I_2 + sL_3 I_3 \end{cases} \quad (5)$$

where V_i and I_i ($i = 1, 2, 3$) are the corresponding voltage of L_i and CM noise current, and L_3 corresponds to L_{CT} in Fig. 2. M_{ij} ($i, j = 1, 2, 3, i \neq j$) are the mutual inductance between windings. I_1 and I_2 are theoretically the same when only CM noise currents are considered, so $I_1 = I_2 = I$. For simplicity, the mutual inductance between the windings can be determined by the theory of transformer. It is because the windings are wound on the same toroid-core and fully coupled together. Hence, simplifying (1), the equivalent CM

impedance of the proposed multi-function common mode choke can be written as

$$\begin{cases} Z_{CM1} = \frac{V_1}{I_1} = s(L_1 + M_{12}) + \frac{s^2 M_{13}(M_{13} + M_{23})}{-sL_{CT} - R_{CT}} \\ Z_{CM2} = \frac{V_2}{I_2} = s(L_2 + M_{21}) + \frac{s^2 M_{23}(M_{13} + M_{23})}{-sL_{CT} - R_{CT}} \end{cases} \quad (6)$$

where Z_{CM1} and Z_{CM2} are the equivalent CM impedance of the multi-function common mode choke, which are almost the same and providing CM noise current reduction.

C. CONSIDERATIONS FOR SELECTING R_{CT} AND TURN RATIO n

In the multi-function common mode choke structure, the magnetizing inductance L , turn ratio n and sense resistor R_{CT} are the dominating parameters which will affect both the two functions of CM noise suppression and CM signal sensing. The equivalent CM impedance of the proposed multi-function common mode choke under different R_{CT} and turn ratio n are shown in Fig. 6-8. It can be observed that when R_{CT} is small, the inductive property of the multi-function common mode choke is diminished. The equivalent CM impedance decreases. When R_{CT} remains constant, the equivalent CM impedance increases as the turn ratio n becomes larger. As for the influence of the magnetizing inductance, it can be seen in Fig. 7 and Fig. 8 that when R_{CT} and the turn ratio n are fixed, the effect of L is not significant, especially for high frequencies. Based on the analysis above, it can be

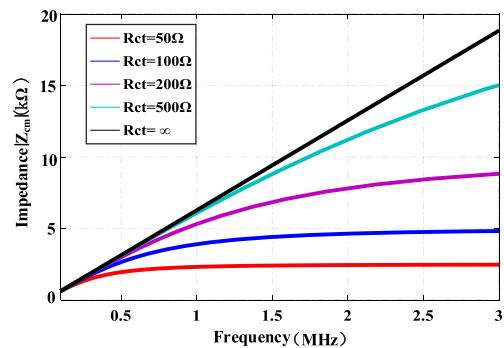


FIGURE 6. Equivalent CM impedance under different R_{CT} when $L_1 = L_2 = 500 \mu H, n = 5$.

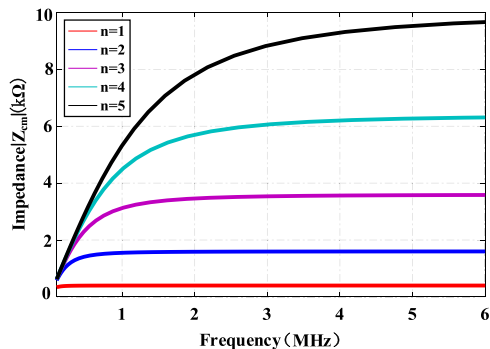


FIGURE 7. Equivalent CM impedance under different n when $L_1 = L_2 = 500 \mu H$, $R_{CT} = 200 \Omega$.

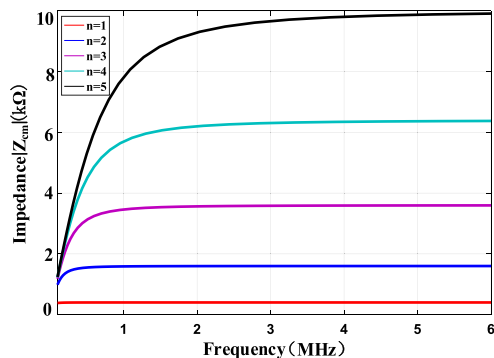


FIGURE 8. Equivalent CM impedance under different n when $L_1 = L_2 = 1000 \mu H$, $R_{CT} = 200 \Omega$.

well known that the larger sense resistor R_{CT} and turn ratio n are preferred when considering the CM noise suppression function in the design of MCMC. But for the CM signal sensing function, it is found that larger sense resistor R_{CT} leads to heavier phase error, which will affect the performance of the active filter. Therefore, there actually exists a tradeoff to consider different factors when designing the parameters of MCMC. Based on the analysis above, the turn ratio and sense resistor R_{CT} are designed to 4:1 and 300Ω , respectively.

IV. NOVEL CM EMI FILTER BASED ON THE PROPOSED MCMC

A. STRUCTURE OF THE NOVEL CM EMI FILTER

In last section, the model of multi-function common mode choke has been developed and analyzed in detail. This part focuses on the active EMI filter based on the proposed MCMC. Fig. 9 shows the structure of the new CM EMI filter using the MCMC. Equivalent CM impedance of the multi-function common mode choke provides CM noise current reduction, which acts as a passive filter. The active part of the new filter is mainly composed of CM signal sensing, an operational amplifier circuit, and RC injection network. The line impedance stabilization network (LISN) is connected between the AC input side and the new CM filter for conductive EMI measurement. The sensing winding (L_{CT})

is used to sense the CM noise current. R_{CT} transforms the sensed CM currents into voltages. The voltages are fed into the op-amp. The output of the amplifier injects cancellation currents through RC network into buses in order to eliminate the electromagnetic interference. Detailed information about this active circuit used in the novel filter can be found in [5], [11] where similar topologies have been discussed extensively. This paper concentrates on the multi-function common mode choke and the novel filter based on it.

B. MODELING OF THE NOVEL FILTER SYSTEM AND STABILITY ANALYSIS

The stability analysis is important and necessary in the new CM filter design, since its operation is based on feedback control. Moreover, the novel CM filter is a new structure. The current signal sensing is not using the conventional current transformer. Therefore, the challenge to design a new EMI filter with high noise attenuation performance on the basis of stability exists. To do that, the system model of the circuit needs to be developed first. Apart from the CM signal sensing model which is discussed previously, the other two parts op-amp circuit and the injection RC network will be presented in this section. the transfer functions of the op-amp and the injection RC network are determined as $G_{amp}(s)$, and $Z_{inj}(s)$, respectively.

As an active circuit component, the op-amp plays a very significant role in the whole filter system. It has a limited frequency bandwidth. An accurate op-amp circuit model, especially for high frequency, helps to better design the whole system and improve the stability. In this paper, a current-feedback amplifier (CFA) is used in the new CM filter. Compared with voltage-feedback amplifier (VFA), the CFA has a wider bandwidth. The wider bandwidth is relatively independent of closed-loop gain, so the constant gain-bandwidth restriction applied to VFAs is removed for CFAs.

In reference [3], a simplified op-amp for VFA was derived, as shown in Fig. 11. In this paper, the model of current-feedback amplifiers (CFA) is presented as shown in Fig. 12. The good thing about CFAs is that they have higher bandwidth as compared to VFAs. Different from the traditional differential amplifier input structure of VFA, the noninverting input of the CFA connects to the input of the buffer, so it has very high impedance. The inverting input connects to the buffer's output, so the inverting input impedance is very low. Z_B is the buffer's output impedance. The current-controlled current source, Z , is a transimpedance. The transimpedance which is usually in the $M\Omega$ range in a CFA serves the same function as gain G_{op} in a VFA.

$$Z_{inj}(s) = \frac{sC}{s^2ESLC + s(R_2 + ESR)C + 1} \quad (7)$$

The closed-loop gain of the op-amp can be derived as shown in (13) with the help of Fig. 12 and Fig. 13, where external gain setting resistors, R_g and R_f , have been added to the circuit. The gains of buffers G_B and G_{out} are

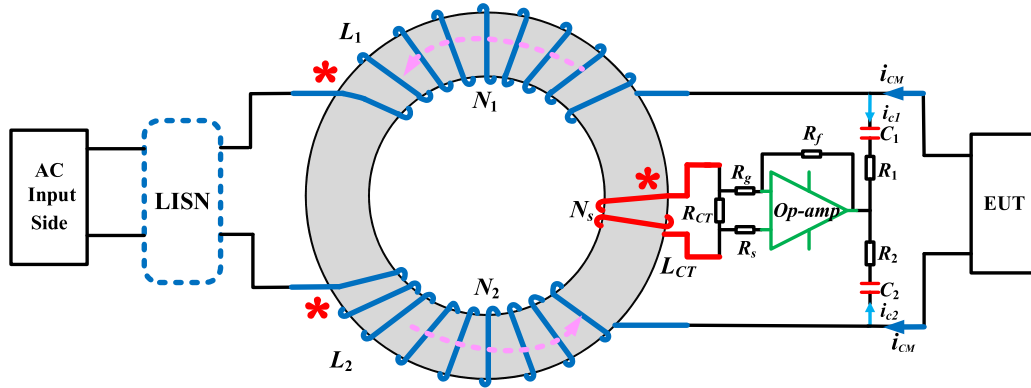


FIGURE 9. Structure of the novel CM filter based on the proposed MCMC.

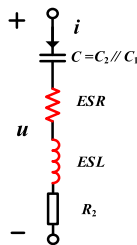


FIGURE 10. Injection network.

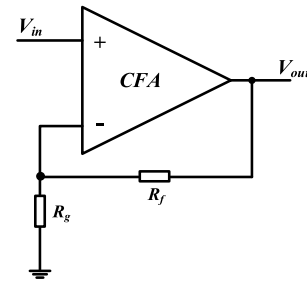


FIGURE 13. High frequency feedback circuit.

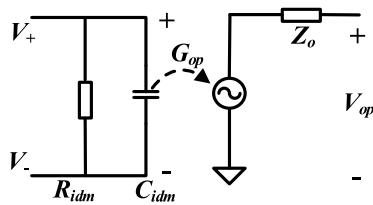


FIGURE 11. Simplified VFA model.

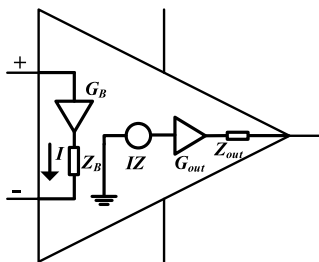


FIGURE 12. The CFA model.

equal one approximately and they can be ignored within the calculations. When the input buffer output impedance, Z_B , approaches zero, equation (8) reduces to equation (9).

$$\frac{V_{out}}{V_{in}} = \frac{\frac{Z(1 + \frac{R_f}{R_g})}{R_f(1 + \frac{Z_B}{R_f \parallel R_g})}}{1 + \frac{Z}{R_f(1 + \frac{Z_B}{R_f \parallel R_g})}} \quad (8)$$

$$\frac{V_{out}}{V_{in}} = \frac{\frac{Z(1 + \frac{R_f}{R_g})}{R_f}}{1 + \frac{Z}{R_f}} = \frac{1 + \frac{R_f}{R_g}}{1 + \frac{Z}{R_f}} \quad (9)$$

$$Z = \frac{Z_0}{(1 + \frac{s}{\omega_1})(1 + \frac{s}{\omega_2})} \quad (10)$$

where Z contains Three parameters, Z_0 , ω_1 , ω_2 . These parameters can be found in the datasheet of an operational amplifier. It can be observed from equation (9) that the accurate closed-loop gain is not equal to ideal closed-loop gain as shown in (11). Therefore, it is important to consider the error term associated with gain when designing the amplification unit. The gain error G_{er} in terms of percentage can be defined and derived as (12), where ‘Actual A_{CL} ’ is given by (9).

$$Ideal\ A_{CL} = 1 + \frac{R_f}{R_g} \quad (11)$$

$$G_{er} = \frac{Ideal\ A_{CL} - Actual\ A_{CL}}{Ideal\ A_{CL}} \times 100\% = \frac{1}{1 + \frac{Z}{R_f}} \times 100\% \quad (12)$$

A model including the noise source, load impedance and the CM filter must be developed to analyze the stability of the new EMI filter. Fig. 14 shows the equivalent circuit for the CM noise for Fig. 9, with a current sensing-current canceling feedback configuration. In Fig. 14, Z_{CM} is the equivalent CM impedance of the multi-function common mode choke

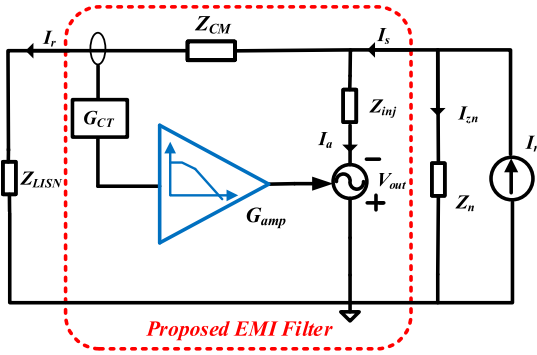


FIGURE 14. Equivalent circuit of the system model.

as shown in equation (7). Note that the input impedance of op-amp in parallel with the sense resistor R_{CT} of the multi-function common mode choke is much larger than R_{CT} . Hence, it is ignored here for simplicity. The Z_{LISN} denotes the LISN' CM impedance. In the model, it is the load of the CM filter. It can be simply modeled as two $50\ \Omega$ resistors in parallel for convenience. I_n and Z_n represent the equivalent CM noise source, which are determined by the power converter. The Norton equivalence is modeled for the noise source. This is because it is convenient to derive transfer functions. $G_{CT}(s)$ is the transimpedance of the current transformer as derived in equation (9). The closed-loop gain of the op-amp $G_{amp}(s)$ is derived in equation (14). $Z_{inj}(s)$ is the impedance of injection RC network as shown in equation (7). The currents flowing through each branch shown in Fig. 14.

Based on Kirchhoff's current law and Kirchhoff's voltage law, equations (13)-(17) can be obtained from Fig.14.

$$I_s(s) = I_a(s) + I_r(s) \quad (13)$$

$$I_n(s) = I_s(s) + I_{zn}(s) \quad (14)$$

$$I_r(s) \times (Z_{CM} + Z_{LISN}) = Z_n \times I_{zn}(s) \quad (15)$$

$$Z_{inj} \times I_a(s) = I_r(s) \times Z_{LISN} + V_{out}(s) \quad (16)$$

$$V_{out}(s) = I_r(s) \times G_{CT}(s) \times G_{amp}(s) \quad (17)$$

From the equations above, the following equations with regard to $I_r(s)$ and $I_a(s)$ can be derived.

$$I_r(s) = (I_n(s) - I_a(s)) \times \frac{Z_n}{Z_n + Z_{CM} + Z_{LISN}} \quad (18)$$

$$I_a(s) = \frac{I_r(s) \times Z_{LISN} + V_{out}(s)}{Z_{inj}} \quad (19)$$

Based on the above equations and the principle of feedback control, the current closed loop signal flow diagram from $I_n(s)$ to $I_r(s)$ can be derived in Fig. 15 [27]. According to the block diagram, the loop gain of the system can be derived by multiplying the forward path gain and feedback path gain as shown in (20), which can be used to evaluate the stability of the system. Fig. 16 shows the calculated loop gain of the designed system. It can be observed from the Bode diagram that the phase margin at the crossover frequency is enough to ensure a stable system. It should be noted that the detailed

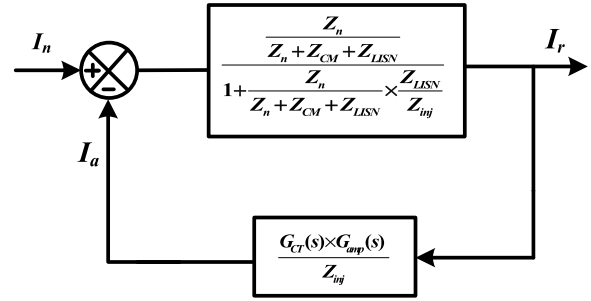


FIGURE 15. Block diagram of the system.

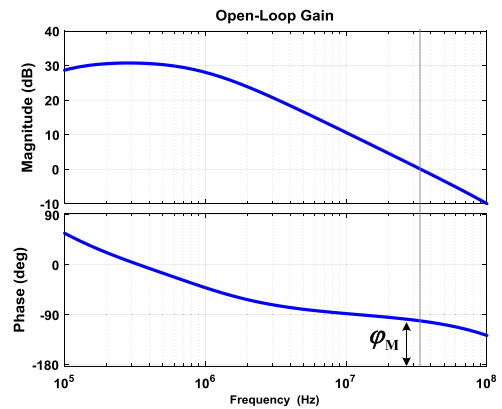


FIGURE 16. Bode diagram of the designed system.

parameters of the designed system are given in section V.

$$G_{open} = \frac{\frac{Z_n}{Z_n + Z_{CM} + Z_{LISN}}}{1 + \frac{Z_n}{Z_n + Z_{CM} + Z_{LISN}} \times \frac{Z_{LISN}}{Z_{inj}}} \times \frac{G_{CT}(s) \times G_{amp}(s)}{Z_{inj}} \quad (20)$$

To validate the performance of the new CM EMI filter based on the proposed MCMC in this paper, insertion loss simulations based on the standard system with a standard interference source are investigated firstly. The filter based on the proposed MCMC is an actual setup same as Fig. 9. A 5-V 100-kHz square wave with $50\ \Omega$ source impedance is used to emulate the noise source. The simulation results are shown in Fig. 17. The red one is the bare noise. The blue one is the result with the filter. It can be observed that the filter achieves high performance noise suppression. For example, the bare noise is 100 dB at 1 MHz. With the filter, the noise reduces to 30 dB.

V. EXPERIMENTS AND VALIDATION

As section II discussed previously, the motivation of the proposed multi-function common mode choke is to combine the CM choke with the current transformer. So that in the hybrid active CM EMI filter design, the current transformer can be removed. Hence, we need to compare the performance of the new CM filter based on the proposed MCMC with the conventional hybrid active CM filter, under the premise that the size of the MCMC is as the same as the traditional

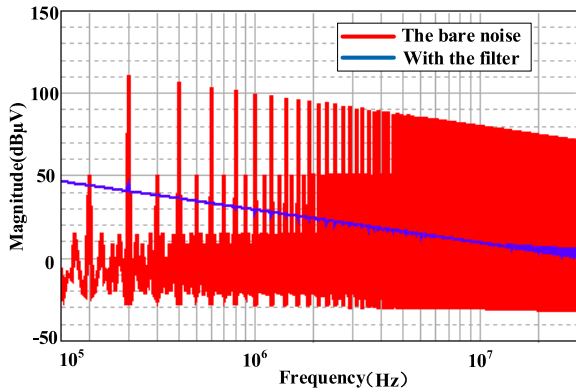


FIGURE 17. Insertion loss simulation results.

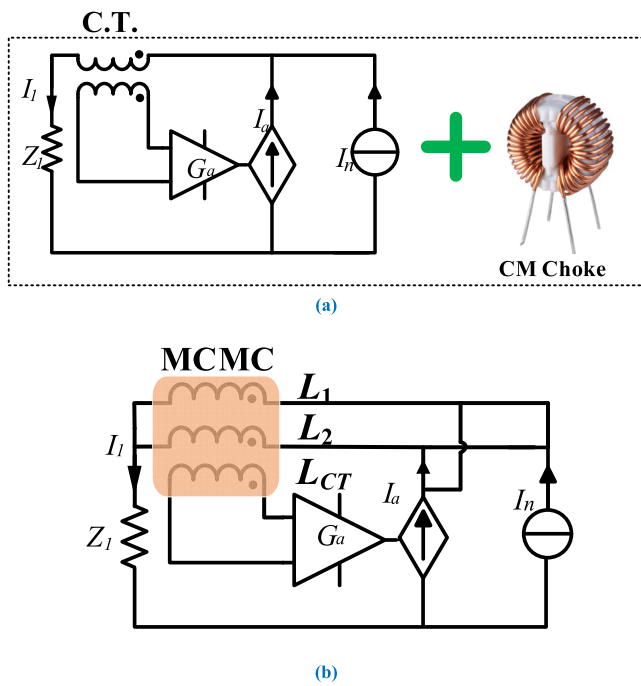


FIGURE 18. Schematics of the two filters: (a) Traditional hybrid active CM EMI filter. (b) New CM EMI filter based on the proposed MCMC.

CM choke. Therefore, the experiments are carried out in two aspects to practically evaluate the proposed technique. One is the performance test of the new filter itself using a standard interference source. Another one is performance comparison between the new filter and the traditional hybrid active filter, which are practically tested on a 100-W commercial AC/DC converter.

The new CM EMI filter based on the multi-function common mode choke and the hybrid active filter were built, and the schematics of the two filters were shown in Fig. 18. For the hybrid active filter, the inductance of the CM choke is 1340 μH . The inductances for the current transformer of the primary winding and the secondary winding are 9.3 μH and 78.5 μH , respectively. The MCMC and the CM choke use the same toroid-core. For the new filter, the multi-function common mode choke consists of two traditional CM inductor

TABLE 2. Key parameters of the active circuits.

	Traditional Filter	New Filter
Sense resistor, R_{CT}	100 Ω	300 Ω
Resistors of the Op-amp, R_g, R_s	1 k Ω	2 k Ω
Feedback resistor of Op-amp, R_f	100 k Ω	51 k Ω
Injection resistors, R_1, R_2	4.7 Ω	4.7 Ω
Injection capacitors, C_1, C_2	100 nF	100 nF

windings (L_1 and L_2) and a CM current sensing winding (L_{CT}). The inductances of L_1 and L_2 are 1332 μH . The inductance of the third sensing winding L_{CT} is 84 μH . The schematic of the filter model is an actual setup same as Fig. 9. Active circuit topologies of the two filters are the same. The key parameters of the active circuits are summarized in Table 2. It should be noted that the design process and optimization of system parameters are based on the previously developed models. For both the traditional hybrid EMI filter and new EMI filter based on the proposed MCMC, the purpose of the design is to achieve the optimal noise suppression on the basis of stability.

A. INSERTION LOSS MEASUREMENT

The new CM EMI filter based on the proposed MCMC is installed in the standard test system to investigate the performance of the new filter itself. A signal generator with 50 Ω impedance is used to the noise source. A 500-mV 100-kHz square wave is fed into the CM filter. The EMI test receiver Rohde&Schwarz ESL3 is used to measure the noise level at the R_{LISN} . For comparison, the spectra of the CM noise without EMI filter and with the EMI filter are measured, respectively. The measurement results are shown in Fig. 19 and Fig. 20. It can be clearly observed that the new CM filter works well for CM noise suppression in the whole test frequency range from 150 kHz to 30 MHz. The filter is able to reduce more than 60 dB at 300 kHz, where is the third harmonic of the noise source. The filter can also provide good noise attenuation at high frequencies. The measurement results well agree with the simulations.

B. PRACTICAL MEASUREMENT WITH THE AC/DC CONVERTER

To demonstrate that the effectiveness of the new CM EMI filter based on the proposed multi-function common mode choke is able to achieve similar EMI noise attenuation compared with the hybrid active EMI filter solution, the two types of filters, as shown in Fig. 18, are practically tested on a 100-W commercial AC/DC converter. The system setup is shown in Fig. 21. For comparison, the place of EMI filter installs the two types of filters to evaluate their performance, respectively. The input and output voltages of the converter are 220 Vac and 24 Vdc, respectively. The LISN provides

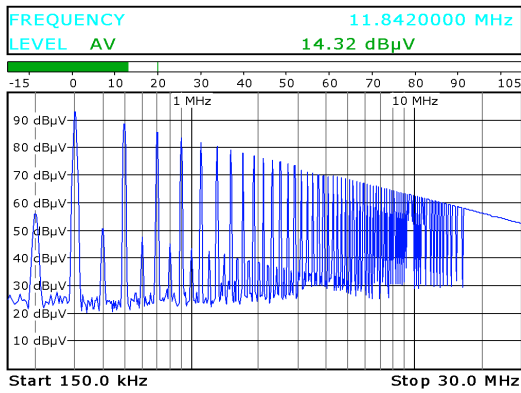


FIGURE 19. Bare noise.

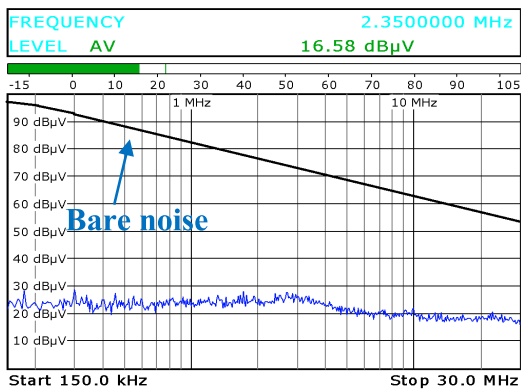


FIGURE 20. CM interference with the new filter.

the standardized impedance and acts as the load of the filters. A CM/DM noise separator is used to extract the CM noise. The noise level is measured by EMI test receiver Rohde&Schwarz ESL3. EN55022 Class B Q.P. conducted EMI standard is adopted in the experiment.

Original passive EMI filters in the commercial AC/DC converter were removed to obtain the bare noise of the converter. The bare noise is measured as shown in Fig. 22(a). It can be seen that the bare CM noise level at the whole

frequency is much high, up to 80-90 dB. In the second experiment, the hybrid active CM EMI filter as shown in Fig. 18(a) is installed into the converter. The CM noise spectra of the converter with the hybrid filter is recorded as shown in Fig. 22(b). The bare CM noise has been significantly attenuated. In the third experiment, the new CM EMI filter based on the proposed MCMC replaces the hybrid active filter, and the measurement result is shown in Fig. 22(c). Compared the bare CM noise level with the noise after using the filters, it can be observed that for the two filters about 50 dB attenuation is achieved at low frequencies and about 40 dB at high frequencies. The performance of the new EMI filter is as good as the hybrid active EMI filter, and it achieves similar EMI noise attenuation with a smaller size than the hybrid active EMI filter solution. The experimental results agree well with the theoretical analysis and the developed models.

The volume of the original passive EMI filter in the commercial AC/DC converter is calculated as 60.61 cm³. Fig. 23 shows the volume comparison of the three types of filters. On the one hand, it can be observed that the size of the EMI filters is greatly reduced by using the active/hybrid filter technology as shown in Fig. 23(a). On the other hand, for the active/hybrid filters, the volume is further reduced from 13.65 cm³ to 9.0 cm³ by applying the proposed technique in this paper, and it achieves 34.1% volume reduction as shown in Fig. 23(b). Therefore, the size of the EMI filters is able to be further reduced to improve system’s power density.

VI. DISCUSSION

A. NO INFLUENCE ON THE DESIGN OF THE DM FILTER

Generally, the CM choke inevitably has some leakage inductance, serving as a DM inductor. Moreover, CM and DM chokes are integrated into a single component to save the space. In the hybrid active CM EMI filter, the design of the CM choke is flexible and can be designed as an integrated inductor or a pure CM inductor as required. Therefore, the questions are raised for the proposed MCMC: Will the

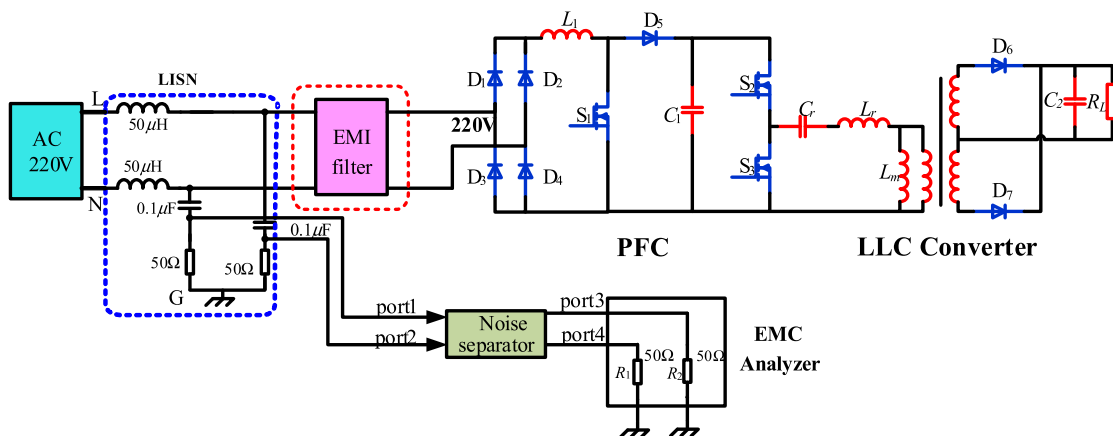
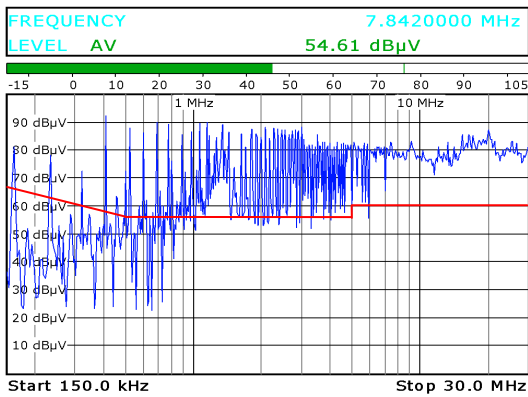
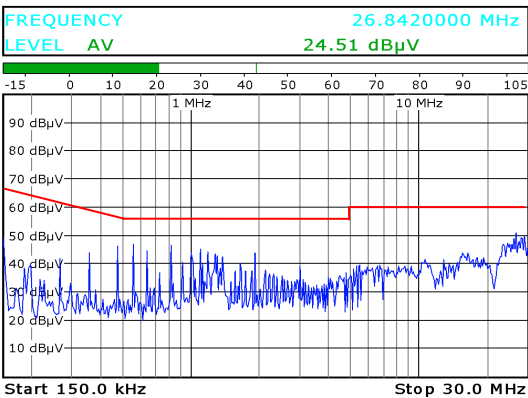


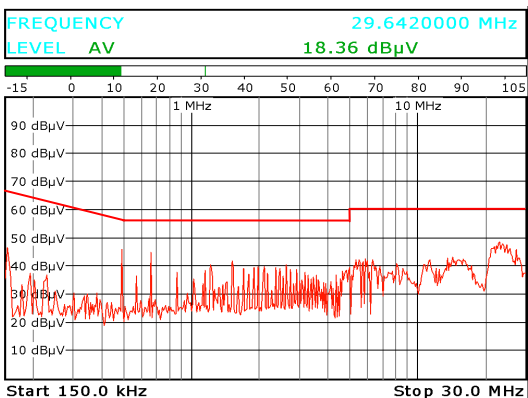
FIGURE 21. Configurations of the experimental setup.



(a)



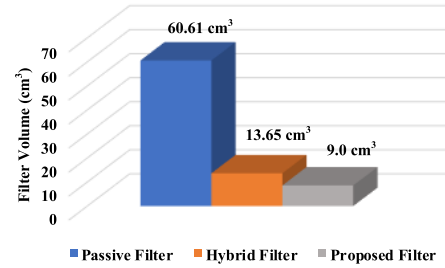
(b)



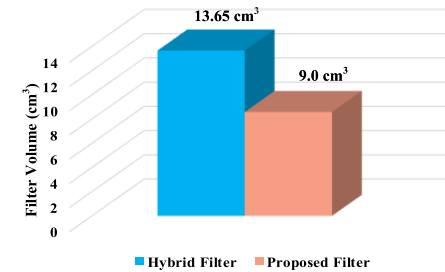
(c)

FIGURE 22. CM noise of the converter: (a) No filter. (b) Using the traditional hybrid active EMI filter. (c) Using the new EMI filter.

new CM EMI filter based on the MCMC proposed in this paper affect the DM signal? Can the leakage inductance of the MCMC act as a DM inductor? In an effort to obtain insight into these questions, the DM noise tests are carried out in experiments. For comparison, the two DM filters are built to investigate the issue. In the experiment, the leakage inductance of the CM choke in the hybrid filter and the MCMC in the new filter act as DM inductors, respectively. The leakage inductance of them are nearly the same measured as 13 μ H. Two 0.47 μ F X capacitors are added to form a CLC configuration. The experimental setup and measurement



(a)



(b)

FIGURE 23. Comparison of the filter volume: (a) Passive EMI filters VS Active EMI filters. (b) Traditional hybrid active filter VS New EMI filter based on the proposed MCMC.

are the same as the experiment of CM noise. The measurement results are shown in Fig. 24. It can be clearly observed that the two DM filters achieve similar noise attenuation, more than 20 dB at high frequencies. The measurement results show that the proposed technique applied in the CM filter has no influence on the design of the DM filter.

B. WINDING BALANCE OF THE MULTI-FUNCTION COMMON MODE CHOKER

In the developed model of the proposed MCMC, it is assumed that the two windings (L_1 and L_2) are identical and symmetrical. The unbalanced impedance of the windings in practical MCMC structure has not been taken into consideration. For the conventional CM choke, magnetic flux induced by DM current is canceled out. But in practice, magnetic saturation may occur when the DM current rapidly increases the flux density due to the unbalanced impedance. This problem also exists in the proposed multi-function common mode choke. On the other hand, since the unbalanced impedance causes the magnetic flux induced by DM current unable to be canceled out, DM signals are converted into CM signals. The CM noise current sensing using the third sensing winding of the MCMC is affected. As a result, the performance of active filter is weakened. Therefore, in the design of the proposed MCMC, high permeability core is used to provide enough saturation flux density to ensure that the magnetic core does not go into saturation. In addition, balanced windings should be ensured as much as possible in the design phase to avoid the problems discussed above. More work focused on the issue of unbalanced impedance will be explored in the future.

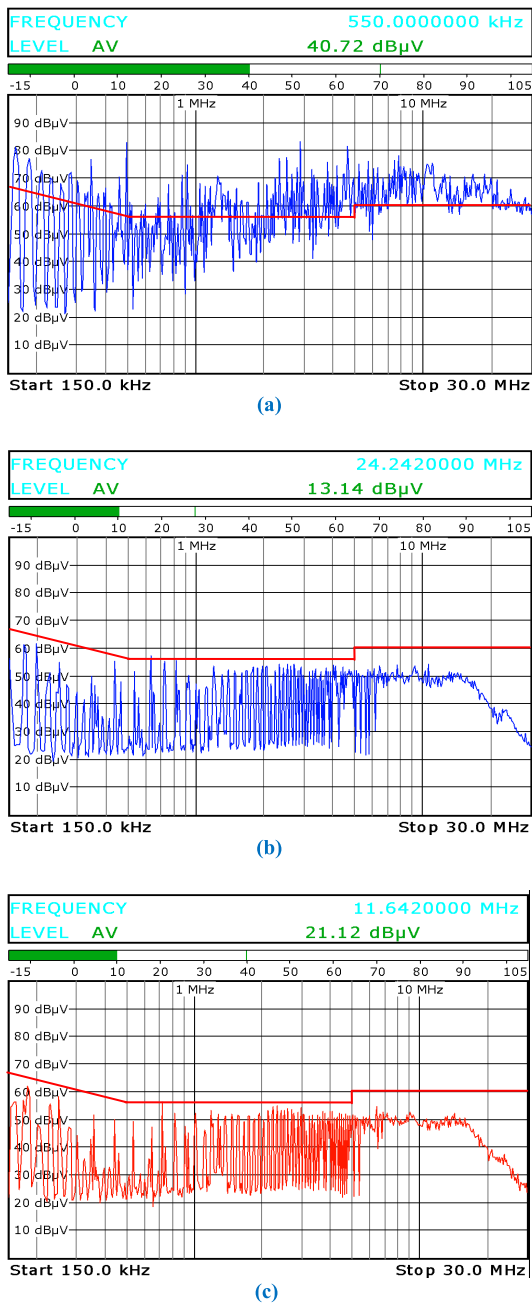


FIGURE 24. DM noise of the converter: (a) No filter. (b) Using the leakage inductance of the traditional CM choke. (c) Using the leakage inductance of the MCMC.

VII. CONCLUSION

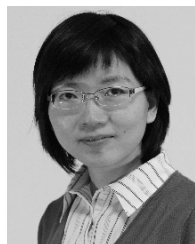
In this paper, a novel multi-function common mode choke is proposed to achieve CM signal sensing and CM noise suppression integrated in a single component. The motivation and structure of the proposed MCMC are first introduced. The models of the two functions are individually developed and explicitly analyzed. Based on the MCMC, a new CM filter is proposed to suppress the noise effectively. The stability of the new filter system is evaluated. To demonstrate the effectiveness of the new CM EMI filter based on the

proposed MCMC, the comparative experiments are carried out between the traditional hybrid active filter and the new filter in a commercial AC/DC converter. The experimental results proved that the new filter using the proposed technique can effectively suppress noise with a smaller size. This proposed technique can reduce the volume, weight and power losses of the EMI filter. It is a novel and practical idea with good potential application value.

REFERENCES

- [1] K. Mainali and R. Oruganti, "Conducted EMI mitigation techniques for switch-mode power converters: A survey," *IEEE Trans. Power Electron.*, vol. 25, no. 9, pp. 2344–2356, Sep. 2010.
- [2] R. P. Clayton, *Introduction to Electromagnetic Compatibility*, 2nd ed. Hoboken, NJ, USA: Wiley, 2006.
- [3] Y. Chu, S. Wang, and Q. Wang, "Modeling and stability analysis of active/hybrid common-mode EMI filters for DC/DC power converters," *IEEE Trans. Power Electron.*, vol. 31, no. 9, pp. 6254–6263, Sep. 2016.
- [4] M. Ali, E. Labouré, F. Costa, and B. Revol, "Design of a hybrid integrated EMC filter for a DC–DC power converter," *IEEE Trans. Power Electron.*, vol. 27, no. 11, pp. 4380–4390, Nov. 2012.
- [5] W. Chen, X. Yang, J. Xue, and F. Wang, "A novel filter topology with active motor CM impedance regulator in PWM ASD system," *IEEE Trans. Ind. Electron.*, vol. 61, no. 12, pp. 6938–6946, Dec. 2014.
- [6] C. Zhu and T. H. Hubing, "An active cancellation circuit for reducing electrical noise from three-phase AC motor drivers," *IEEE Trans. Electromagn. Compat.*, vol. 56, no. 1, pp. 60–66, Feb. 2014.
- [7] M. C. Di Piazza, A. Ragusa, and G. Vitale, "An optimized feedback common mode active filter for vehicular induction motor drives," *IEEE Trans. Power Electron.*, vol. 26, no. 11, pp. 3153–3162, Nov. 2011.
- [8] Y.-C. Son and S.-K. Sul, "Generalization of active filters for EMI reduction and harmonics compensation," *IEEE Trans. Ind. Appl.*, vol. 42, no. 2, pp. 545–551, Mar. 2006.
- [9] M. Ali, E. Labouré, and F. Costa, "Integrated active filter for differential-mode noise suppression," *IEEE Trans. Power Electron.*, vol. 29, no. 3, pp. 1053–1057, Mar. 2014.
- [10] N. K. Poon, J. C. P. Liu, C. K. Tse, and M. H. Pong, "Techniques for input ripple current cancellation: Classification and implementation," *IEEE Trans. Power Electron.*, vol. 15, no. 6, pp. 1144–1152, Nov. 2000.
- [11] W. Chen, X. Yang, and Z. Wang, "A novel hybrid common-mode EMI filter with active impedance multiplication," *IEEE Trans. Ind. Electron.*, vol. 58, no. 5, pp. 1826–1834, May 2011.
- [12] M. C. Di Piazza, M. Luna, and G. Vitale, "EMI reduction in DC-fed electric drives by active common-mode compensator," *IEEE Trans. Electromagn. Compat.*, vol. 56, no. 5, pp. 1067–1076, Oct. 2014.
- [13] A. C. Chow and D. J. Perreault, "Design and evaluation of a hybrid passive/active ripple filter with voltage injection," *IEEE Trans. Aerosp. Electron. Syst.*, vol. 39, no. 2, pp. 471–480, Apr. 2003.
- [14] D. Shin et al., "Analysis and design guide of active EMI filter in a compact package for reduction of common-mode conducted emissions," *IEEE Trans. Electromagn. Compat.*, vol. 57, no. 4, pp. 660–671, Aug. 2015.
- [15] D. Shin, S. Jeong, and J. Kim, "Quantified design guidelines of a compact transformerless active EMI filter for performance, stability, and high voltage immunity," *IEEE Trans. Power Electron.*, vol. 33, no. 8, pp. 6723–6737, Aug. 2018.
- [16] S. Wang, Y. Y. Maillet, F. Wang, D. Boroyevich, and R. Burgos, "Investigation of hybrid EMI filters for common-mode EMI suppression in a motor drive system," *IEEE Trans. Power Electron.*, vol. 25, no. 4, pp. 1034–1045, Apr. 2010.
- [17] M. C. Di Piazza, A. Ragusa, and G. Vitale, "Effects of common-mode active filtering in induction motor drives for electric vehicles," *IEEE Trans. Veh. Technol.*, vol. 59, no. 6, pp. 2664–2673, Jul. 2010.
- [18] J. Biela, A. Wirthmueller, R. Waespe, M. L. Heldwein, K. Raggl, and J. W. Kolar, "Passive and active hybrid integrated EMI filters," *IEEE Trans. Power Electron.*, vol. 24, no. 5, pp. 1340–1349, May 2009.
- [19] D. Hamza, M. Qiu, and P. K. Jain, "Application and stability analysis of a novel digital active EMI filter used in a grid-tied PV microinverter module," *IEEE Trans. Power Electron.*, vol. 28, no. 6, pp. 2867–2874, Jun. 2013.

- [20] D. Hamza and M. Qiu, "Digital active EMI control technique for switch mode power converters," *IEEE Trans. Electromagn. Compat.*, vol. 55, no. 1, pp. 81–88, Feb. 2013.
- [21] D. Hamza, M. Pahlevaninezhad, and P. K. Jain, "Implementation of a novel digital active EMI technique in a DSP-based DC–DC digital controller used in electric vehicle (EV)," *IEEE Trans. Power Electron.*, vol. 28, no. 7, pp. 3126–3137, Jul. 2013.
- [22] D. Zhang, D. Y. Chen, M. J. Nave, and D. Sable, "Measurement of noise source impedance of off-line converters," *IEEE Trans. Power Electron.*, vol. 15, no. 5, pp. 820–825, Sep. 2000.
- [23] N. Kondrath and M. K. Kazimierczuk, "Bandwidth of current transformers," *IEEE Trans. Instrum. Meas.*, vol. 58, no. 6, pp. 2008–2016, Jun. 2009.
- [24] X. Chang, W. Chen, Y. Yang, K. Wang, and X. Yang, "Research and realization of a novel active common-mode EMI filter," in *Proc. IEEE Appl. Power Electron. Conf. Expo. (APEC)*, Mar. 2015, pp. 1941–1945.
- [25] D. Hamza, M. Sawan, and P. K. Jain, "Suppression of common-mode input electromagnetic interference noise in DC-DC converters using the active filtering method," *IET Power Electron.*, vol. 4, no. 7, pp. 776–784, Aug. 2011.
- [26] W. Chen, W. Zhang, X. Yang, Z. Sheng, and Z. Wang, "An experimental study of common- and differential-mode active EMI filter compensation characteristics," *IEEE Trans. Electromagn. Compat.*, vol. 51, no. 3, pp. 683–691, Aug. 2009.
- [27] R. Goswami and S. Wang, "Modeling and stability analysis of active differential-mode EMI filters for AC/DC power converters," *IEEE Trans. Power Electron.*, vol. 33, no. 12, pp. 10277–10291, Dec. 2018.
- [28] F. Luo, D. Dong, D. Boroyevich, P. Mattavelli, and S. Wang, "Improving high-frequency performance of an input common mode EMI filter using an impedance-mismatching filter," *IEEE Trans. Power Electron.*, vol. 29, no. 10, pp. 5111–5115, Oct. 2014.
- [29] W. Chen, X. Yang, and Z. Wang, "An active EMI filtering technique for improving passive filter low-frequency performance," *IEEE Trans. Electromagn. Compat.*, vol. 48, no. 1, pp. 172–177, Feb. 2006.
- [30] Y. Chu and S. Wang, "A generalized common-mode current cancellation approach for power converters," *IEEE Trans. Ind. Electron.*, vol. 62, no. 7, pp. 4130–4140, Jul. 2015.
- [31] S. Wang, Y. Y. Maillet, F. Wang, R. Lai, F. Luo, and D. Boroyevich, "Parasitic effects of grounding paths on common-mode EMI filter's performance in power electronics systems," *IEEE Trans. Ind. Electron.*, vol. 57, no. 9, pp. 3050–3059, Sep. 2010.
- [32] Y. Sha, W. Chen, H. Qi, Y. Han, C. Pei, and Y. Zhu, "A study of an active EMI filter for high current ACDC converter," in *Proc. IEEE 3rd Int. Future Energy Electron. Conf. Asia (ECCE)*, Jun. 2017, pp. 1797–1799.
- [33] R. Goswami, S. Wang, and Y. Zhang, "Modeling, analysis and design of differential mode active EMI filters with feedforward and feedback configurations for AC-DC converters," in *Proc. IEEE Energy Convers. Congr. Expo. (ECCE)*, Sep. 2016, pp. 1–8.
- [34] Y. Chu, S. Wang, N. Zhang, and D. Fu, "A common mode inductor with external magnetic field immunity, low-magnetic field emission, and high-differential mode inductance," *IEEE Trans. Power Electron.*, vol. 30, no. 12, pp. 6684–6694, Dec. 2015.



WENJIE CHEN received the B.S., M.S., and Ph.D. degrees in electrical engineering from Xi'an Jiaotong University, Xi'an, China, in 1996, 2002, and 2006, respectively. From 2012 to 2013, she was a Visiting Scholar with the Department of Electrical Engineering and Computer Science, The University of Tennessee, Knoxville, TN, USA. She then came back to Xi'an Jiaotong University and engaged in the teaching and researches in power electronics. Since 2002, she has been a member with the School of Electrical Engineering, Xi'an Jiaotong University, where she is currently a Professor. Her main research interests include electromagnetic interference, active filters, and power electronic integration.



XU YANG received the B.S. and Ph.D. degrees in electrical engineering from Xi'an Jiaotong University, Xi'an, China, in 1994 and 1999, respectively. From 2004 to 2005, he was a Visiting Scholar with the Center of Power Electronics Systems (CPES), Virginia Polytechnic Institute and State University, Blacksburg, VA, USA. He then came back to Xi'an Jiaotong University and engaged in the teaching and researches in power electronics and industrial automation area. Since 1999, he has been a member with the School of Electrical Engineering, Xi'an Jiaotong University, where he is currently a Professor. His research interests include soft switching topologies, pulse width modulation (PWM) control techniques, power electronic integration, and packaging technologies.



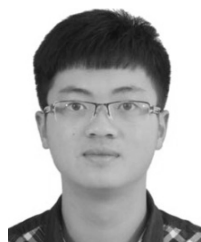
MINGHUA ZHENG received the B.S. degree in electrical engineering from the University of Shanghai for Science and Technology, Shanghai, China, in 2008. He is currently pursuing the M.S. degree with Fuzhou University, Fuzhou, China. He is also a Senior Engineer with Omron (China) Ltd. His current research interests include electromagnetic interference active filters.



YANG YANG received the B.S. degree in electrical engineering from Nanjing Agricultural University, Nanjing, China, in 2017. She is currently pursuing the M.S. degree with Xi'an Jiaotong University, Xi'an, China. Her current research interests include wireless power transfer and electromagnetic interference.



RUI WANG received the B.S. degree in electrical engineering from Xi'an Jiaotong University, Xi'an, China, in 2017, where he is currently pursuing the M.S. degree in power electronics with the School of Electrical Engineering. His research interests include sound field optimization and active noise reduction technology for the filtering field of converter station.



LIYU DAI received the B.S. degree in electrical engineering from Fuzhou University, Fuzhou, China, in 2017. He is currently pursuing the M.S. degree in power electronics with the School of Electrical Engineering, Xi'an Jiaotong University. His research interests include electromagnetic interference and active filters.